Conf-810836--3

CONF-810836--3

DE83 009630

# SOME REMAINING PROBLEMS IN HCDA ANALYSIS

by

Y. W. Chang
Engineering Mechanics Program
Reactor Analysis and Safety Division
Argonne National Laboratory
Argonne, Illinois 60439, U.S.A.

## 1. Introduction

The safety assessment and licensing of liquid-metal fast breeder reactors (LMFBRs) requires an analysis on the capability of the reactor primary system to sustain the consequences of a hypothetical core-disruptive accident (HCDA). One way to achieve this is to use the basic conservation equations of mass, momentum, and energy, together with the equations of state of the reactor materials to calculate the response of the reactor primary system under the postulated nuclear excursion condition analytically. In recent years, the development of high-speed large computers has made it feasible to use computer programs to solve these equations numerically. Computer programs have been developed and are used by most fast reactor projects to study the response of primary containment to HCDAs.

Although computational methods and computer programs developed for HCDA analyses can predict reasonably well the response of the primary containment system, and follow up the phenomena of HCDA from the start of excursion to the time of dynamic equilibrium in the system, there remain areas in the HCDA analysis that merit further analytical and experimental studies. These are the analysis of fluid impact on reactor cover, three-dimensional analysis, the treatment of the perforated plates, material properties under high strain rates and under high temperatures, the treatment of multifield flows, and the treatment of prestressed concrete reactor vessels. The purpose of this paper

is to discuss the structural mechanics of HCDA analysis in these areas where improvements are needed.

## 2. Fluid Impact on Reactor Cover

Fluid impact is one of the problems in the HCDA analysis which needs improvement. The difficulty of the fluid impact calculation is due to (1) the fluid cavitation and (2) the spatial discretization in the numerical treatment in defining the impact.

When a pressure wave emanating from the reactor core arrives at the free surface of the coolant, it reflects back into the coolant as a tension wave. As the tension wave passes through the coolant, it cavitates the fluid and throws off a spray of coolant towards the reactor cover. This spray of coolant produces a pressure loading on the reactor cover as it impacts on the cover. When the main body of coolant moving upwards strikes the reactor cover, it produces another pressure loading on the cover. This second pressure loading is often referred to as the fluid impact load. Obviously, the impact load delivered to the reactor cover depends on the cavitation model and the equation of state used to describe the behavior of the cavitated fluid. Unfortunately, the fluid cavitation phenomenon is often ignored in the numerical analysis.

One common approach for treating the fluid cavitation is to allow the fluid to take some negative pressures. Usually a pressure cut-off point is defined on the P-V curve. Once the pressure cut-off point is reached, further expansion in fluid volume does not affect the fluid pressure, the pressure remains at the cut-off value until the fluid recompacts. This model is often referred to as the "$p_{min}$" model. It ignores energy dissipation from the growth and collapse of cavitated bubbles. Theoretically, the negative

pressure cut-off point should correspond to the tensile strength of the fluid. However, the values used for the "$p_{min}$" model are often too large and have no physical justification. Another approach is to provide a hysteresis loop in the P-V curve to account for the energy losses due to the growth and collapse of cavitated bubbles. The pressure histories obtained with a hysteresis loop P-V models are in general more smooth and less spiky than those of the "$p_{min}$" model, particularly, during the time when the fluid is being recompressed.

Recently, Jones [1] used the Rayleigh-Plesset equation

$$R\ddot{R} + \frac{3}{2}\dot{R}^2 = \frac{1}{\rho}\left(p_i - p_\infty - \frac{2\sigma}{R} - 4\frac{\nu\dot{R}}{R}\right) , \qquad (1)$$

to study the effects of the cavitated bubbles on containment loading; here R is the radius of the cavitated bubbles, $\rho$ the liquid density, $p_i$ the bubble internal pressure, $p_\infty$ the pressure at infinity, $\sigma$ the surface tension, and $\nu$ the viscosity. If Eq. (1) is solved together with the conservation equations of fluid mass, momentum and energy and equation of state, not only the growth and collapse of the cavitated bubbles can be determined, but also the effects of the radial motion of the fluid around the cavitation bubbles can be included in the containment analysis. The fluid impact loads obtained with this type of analysis should be more realistic and have less numerical oscillations. This type of cavitation model should be used to study the behavior of the cavitated bubbles together with an equation of state which relates the bubble internal pressure with its volume changes. If these models prove effective, they should be incorporated into the containment codes.

In the HCDA analysis, the fluid is often treated as inviscid and time integrations are performed explicitly. Since the fluid model neglects both tensile and viscous forces, cavitations and voids which are physically unreal can

occur in the computational meshes when they expand after the passage of a tension wave. This expansion can continue indefinitely if there are no compressed zones in the surrounding meshes to arrest its motion. As a result, cavitations and voids are formed in the computational meshes. Explicit time integration calculation further aggravates this situation since the mass conservation is satisfied only locally, that is meshwisely, in an explicit time integration scheme.

Another phenomenon associated with fluid cavitation is the pressure oscillations in the impact meshes. In the numerical analysis, the fluid domain is subdivided into discrete meshes. When a surface mesh impacts on the reactor cover, a large impact pressure is developed in the mesh which impacts the cover. If the fluid mesh underneath the impact mesh contains voids, it will act like a free surface and reflect back a rarefaction wave into the impact mesh. The pressure in the impact mesh will decrease very quickly and often drop to zero in a relatively short period of time. However, as the mesh underneath the impact mesh is being compressed by the remaining upward-moving fluid, a pressure pulse similar to that of the initial impact pressure of the impact mesh can be developed in the compressed mesh. This newly developed pressure pulse can cause the pressure in the impact mesh to rise again. However, this pressure will drop to zero, if another rarefaction wave reflects back from a mesh which contains voids. This type of pressure oscillation will repeat for a number of times until all the voids in the computational meshes created by the tension wave have been compressed to negligibly small volumes or totally removed.

Since continuity requirements are implied in the implicit solution, the implicit method has a tendency to distribute cavitation and voids uniformly to the whole fluid domain. As a result, the solution obtained with implicit time

integration often shows fewer pressure oscillations. Figure 1 shows two pressure plots obtained with the REXALE-3D computer code [2]. One calculation used the implicit time integration scheme and the other used the explicit time integration scheme. As can be seen from these figures, the use of the implicit time integration scheme can eliminate some of the pressure oscillations created by physically unrealistic fluid cavitation. Similarly, the use of artificial viscosities, particularly the linear viscosity, can eliminate some of the physically unrealistic fluid cavitation. Since the "$p_{min}$" model allows the fluid to have some tensile strength, it can also reduce some of the pressure oscillations.

Another difficulty encountered in the treatment of fluid impact is the severe noise introduced by the spatial discretization. When a fluid surface impacts a structure, the contact area grows continuously with time. In the numerical procedure, this continuous contact is represented by a series of discrete contacts. In computer codes, impact of a fluid mesh on the reactor cover is often arbitrarily defined as occurring when more than half the fluid surface of that mesh is in contact with the reactor cover. This is a reasonable assumption for a moving fluid whose surface is relatively flat, because the time from the first impact of fluid in a given mesh to the full contact is very short. For a curved surface, however, there is a long period of time between the first impact of the fluid to the time when impact is completed. Thus, the continuous impact is represented by a series of discrete impacts, each of which is associated with a spike in the impact force.

These spikes are caused by spatial discretization and discontinuities in the fluid velocity. In the first period, when the fluid is in contact with the reactor cover, it should be gradually compressing. But impact has not been defined and no pressure calculation is made in the numerical procedure.

When half of the mesh is in contact with the reactor cover, the impact is defined to occur. Suddenly the momentum of the whole top surface of the fluid in that mesh is set to zero and a pressure calculation is performed as if the whole mesh had impacted. In fact, at this point, only about half the surface has impacted and the other half is still free. Obviously, this treatment causes sudden sharp pressure spikes.

Since the normal velocities of the fluid before and after the impact are not equal, a step discontinuity in velocity can cause a sudden increase in fluid pressure. In addition, the semi-discretization of the fluid and structure alters the character of the impact from a spatially smooth phenomenon characterized by a continuous contact to a series of discrete impacts. Belytschko and Mullen [3] have proposed an impact regularization scheme for incompressible fluid. They imposed certain conditions on the fluid surface. The following is a brief description of their technique.

Consider a smooth fluid surface partially in contact with the structural surface. Let the unit normals to the fluid surface and structural surface be $n_i^F$ and $n_i^S$, respectively, and the distance between the fluid and structural surfaces measured along the unit normal to the structural surface by $\varepsilon$. The *boundary conditions imposed on the fluid surface are:*

$$(1-\kappa)\left[\frac{v_i^{S,k}\, n_i^{S,k} + \xi\, v_i^{F,k}\, n_i^{S,k}}{1+\xi} - v_i^{F,k+1}\, n_i^{S,k}\right]\gamma + \kappa\, p^{F,k+1} = 0 \quad \text{for} \quad 0 < \kappa \leq 1 , \tag{2}$$

$$v_i^{F,k+1}\, n_i^S = v_i^{S,k+1}\, n_i^S \quad \text{for} \quad \kappa = 0 , \tag{3}$$

$$p^{F,k+1} - p^{S,k+1} = 0 \quad \text{for all } \kappa , \tag{4}$$

where $\kappa=\varepsilon/\delta$ for $0 < \varepsilon < \delta$; $\kappa=0$ for $\varepsilon \leq 0$; $\kappa=1$ for $\varepsilon \geq \delta$; v is the velocity; p is the pressure; superscript k denotes the time cycle; and $\delta$, $\xi$, and $\gamma$ are parameters selected by the analysts. If $\delta$ is set equal to the mesh size in the fluid, the smoothing domain adjacent to the structure is one mesh length in depth.

Equation (2) is used as a boundary condition on the fluid surface when $0 < \kappa \leq 1$. When $\kappa$ is close to 1.0, Eq. (2) imposes a near zero pressure condition on the fluid surface. As $\kappa$ decreases, the first term becomes dominant, forcing the fluid velocity to an intermediate velocity. When $\kappa=0$, the fluid nodes are in contact with the structure, the normal velocity condition, Eq. (3) applies. When $\kappa=1$, Eq. (2) enforces a zero pressure condition on the fluid surface. In all cases, Eq. (4) is imposed on the structure.

The form of Eq. (2) was motivated by the conditions of plastic impact of rigid bodies. If a mass $m^F$ collides with a mass $m^S$, then the velocity $v^+$ after impact is given by

$$\frac{m^S v^S + m^F v^F}{m^S + m^F} - v^+ = 0 \ . \tag{5}$$

Letting $\xi = \frac{m^F}{m^S}$, Eq. (5) becomes

$$\frac{v^S + \xi v^F}{1+\xi} - v^+ = 0 \ , \tag{6}$$

which is the quantity in the parenthesis of the first term of Eq. (2), so that it can be viewed as a predictor based on plastic impact. This type of regularization procedure for incompressible fluid can eliminate the spurious noise which accompanies the discrete impacts of nodes due to spatial

discretization. It should be generalized to include the compressibility of fluid and to apply to the HCDA analysis. It is believed that the spurious noise in fluid impact pressures obtained from the numerical analysis can be eliminated if the containment codes used for the fluid impact analysis include a realistic fluid cavitation model and an impact regularization scheme. Implicit time integration may also be of benefit of its better treatment in fluid impact calculation, this option should be available in the containment codes.

## 3. Three-Dimensional Analysis

One of the main concerns in the HCDA analysis is the ability of the primary system to maintain its structural integrity under accident conditions. Containment codes developed for HCDA analysis are almost all two-dimensional. These computer codes have beer used very successfully for loop-type of reactors because these type of reactors can easily lend themselves to an axisymmetric configuration. However, this is not the case for the pool-type of reactor. The pool-type of LMFBR is designed with the entire primary coolant system, such as primary pumps and intermediate heat exchangers, contained within a primary tank. It is primarily the inclusion of these components within the primary tank that precludes the use of the 2-D containment codes. Therefore, to realistically analyze the response of a pool-type reactor under HCDA conditions, a coupled hydrodynamic structural analysis must be performed in three-dimensions. However, there are difficulties in 3-D analysis. Some of these problems are discussed below.

Computer running times and memory requirements of 3-D analyses are two of the major obstacles in the use of 3-D containment codes. One-dimensional problems with very high resolution can be accomplished at nominal cost with

small memory requirements. Manpower costs to set up and perform one-dimensional calculations are also small. Two-dimensional calculations require substantial greater resources. Containment problems with 5000 meshes can be easily accommodated on CDC 7600 and IBM 370 computers. In fact, problems of this size are ran routinely at many large research laboratories. Three-dimensional calculations are quite different; they require large core memory storage and considerable amount of CPU time.

Table 1 compares the computer core storage and CPU times required for 2- and 3-D calculations. The problem chosen for this comparison is a simple coolant slug impact problem. The model consists of a column of coolant contained in a circular cylindrical vessel. Before the slug impact, the coolant is assumed to move upward with a uniform velocity. The mathematical model for 2-D calculations has 6 zones in the radial direction and 12 zones in the axial direction. The 3-D calculation uses a quarter of the cross section to illustrate how the cross section should be discretized. To achieve the same degree of resolution, this quarter cross section of the slug is divided into 27 zones. Same number of zones are used in the axial direction. The total number of fluid elements is 324. As can be seen, the increase in the CPU time for a 3-D calculation is surprisingly large. The ratio of the CPU times for 2- and 3-D calculations for performing one mesh-cycle computation is about 1 to 8; the ratio of core storage for one fluid mesh is about 1 to 3. If a reactor is assumed to have three loops, the 3-D analysis can be performed with a 120° sector. With the numbers given in Table 1, it would require 432 fluid zones to complete the model. The CPU time for a 3-D analysis would be 50 times as great as a 2-D analysis.

Figure 2 is a sector model of a pool reactor, which includes a sector of the rotating plug assembly, deck structure, support skirt, in-tank component,

primary tank, sodium pool, core region, and core support structure. It is modeled with 450 hexahedrons and 477 plate elements. The model has 948 nodes and requires 1100K of storage on IBM 370 computers. The CPU time for 3000 cycles of calculations is 2.3 hours. If $\Delta t$ is taken to be 50 μs, the excursion time at the end of 3000 cycle calculation is 150 ms. For a problem with no sectional symmetry, it often requires several thousands of hexahedron elements and plate elements to complete the model. The computer core storage and CPU time can then become prohibitive in an HCDA analysis. For example, for a 15x15x30 meshes, about 3000K core storage in IBM 370 computer and about 15 hours of CPU time are required to complete 1000 time steps. Resolutions comparable to those attained routinely with two-dimensional problems are at least an order of magnitude beyond current feasible resources in both computer running times and memory requirements.

Another problem which confronts the analysts in the 3-D analysis is the unreal numerical oscillations which are caused by the method of solution rather than the physics of the problem. For example, the frequently occurring "hourglass" distortions in a quadrilateral mesh in two-dimensional analysis are not physically real. They are the nontrivial homogeneous solutions of the strain equations. In three-dimensional analysis, the commonly used hexahedron fluid element (6-face 8-node) has 24 degrees of freedom, but only six strain equations. Of the 24 degrees of freedom, six are rigid-body motions (three translations and three rotations), which do not increase strains of the element. *Therefore, there are 18 independent variables in six equations.* As a result, there exist 12 sets of linearly independent nontrivial homogeneous solutions, which are mathematically possible but physically unreal. In other words, 12 different modes of hourglass distortion can exist in a hexahedron fluid element under certain conditions. Once these modes of distortions are

initiated, the nodes of the element move in and out alternately in such a way that the volume of the element remains unchanged and no restoring force is activated. Thus a scheme must be used to control or regulate these distortions.

Three schemes are commonly used in two-dimensional analysis to control the nonphysical oscillations: the rotational q method; the triangular q method; and the alternate-node coupling method. However, extending these methods to three dimensions become extremely complicated. For instance, the triangular q method developed by Milkins [4] for the hexahedron element involves considerable coding and computation. The hexahedron element must be replaced by tetrahedrons, and the velocity derivatives of each tetrahedron must be calculated and stored separately in the computer memory storage. Furthermore, the hourglass qs used in these methods are not independent of the deformation and rigid body modes of the element, which could degrade the solution.

The first work to pursue the orthogonality of the hourglass modes to the first order modes was that of Kosloff and Frazier [5]. They divided the 24 modes into one translation mode, three constant displacement-gradient modes and four hourglass modes for each coordinate direction. Figure 3 shows four hourglass modes of a unit cube in a natural coordinate system $(\xi,\eta,\zeta)$. These modes have displacements only along the $\xi$-axis. Each mode will contribute a force to the node and the total force is the sum of the contributions of each mode. Similar modes would occur in the $\eta$- and $\zeta$-axis. As can be seen, their method involves a considerable amount of coding and computation. It also requires the solution of four sets of eight equations for each element at every time step during the transient analysis.

Recently, Flanagan and Belytschko [6] developed a technique which isolates the hourglass modes from the rigid body and uniform strain modes. Their algo-

rithm is simple and elegant; only 20-30 FORTRAN statements are needed for both the evaluation of the internal and anti-hourglass nodal forces. There are two forms of hourglass control available in their scheme: viscous control and elastic control. In the viscous control method, artificial damping force is used to combat the hourglass modes. It allows some hourglassing but can prevent violent oscillations. In the elastic control method, artificial stiffness is used to combat the hourglass modes. This method allows only mild hourglassing and is found to be more effective in achieving mesh stability.

The important aspects of this technique are: (1) hourglass shapes are orthogonal to the uniform strain and rigid body modes; (2) the shape vectors are computed directly, i.e., no solution of equations is necessary; and (3) the volume and uniform strain states of a hexahedron are integrated accurately without an averaging scheme. This type of hourglass control scheme should receive further study and be implemented in 3-D containment codes to improve their accuracy and stability in numerical computations, in addition to achieving substantial savings in computation time.

## 4. Treatment of the Perforated Dip Plate

Recent studies show that the perforated dip plate can play an important role in the overall containment response; in particular, it has a mitigating effect on the slug impact and upper vessel deformation. Figure 4 is the mathematical model of a reactor used in the ANL study [7]. It consists of a primary vessel, a core barrel, a perforated dip plate, and a reactor cover. Marker particles are used here to aid in the visualization of the coolant movement. Two calculations were performed: one with the perforated dip plate and the other without.

Figures 5 and 6 show the configuration of the reactor at three different times with and without the perforated dip plate, respectively. It is evident that the perforated dip plate has the effect of (1) confining the HCDA bubble expansion, (2) slowing down the upward movement of the coolant slug, (3) changing the smooth coolant free surface to a relatively turbulent one, and (4) reducing the slug-impact loads and upper vessel wall deformation. Yet, the increase in core barrel deformation due to the slower core-gas bubble expansion which results from the suppression effect of the perforated dip plate is still quite small.

As can be seen, the perforated dip plate model used in the analysis is rather simple. The perforated holes were lumped together into three annular holes where only the total flow area of the perforated holes was conserved and the calculations were performed with a small number of computational meshes. Moreover, the motion of fluid was calculated by the two-dimensional Navier-Stokes equations for laminar flows. Obviously, this type of modeling and treatment is not adequate, if one wants to take the full advantage of the perforated dip plate in the HCDA analysis.

However, from the applications point of view, it is necessary to use a small number of computational meshes for the modeling of the perforated dip plate. Of course, to use several times as many meshes may produce resolution of fine details of the flow, but they are of no interest in the HCDA analysis. One can even build a three-dimensional model for the perforated dip plate, but it would require many more meshes. The number of meshes required may exceed the limit of the computer memory. Even if it does not exceed the limit of the computer memory, it would be difficult, if not impossible, to obtain solutions within the computer time available to most users.

Therefore, it is necessary to use a small number of meshes to model the perforated dip plate. As a matter of fact, it is the use of relatively few meshes which contributes a large measure to the practicality of computer codes in the HCDA analysis. However, treating the turbulent jets as laminar flows and ignoring the energy loss due to contraction and expansion may introduce errors in the numerical results. Therefore, a better approach is to develop a perforated dip plate model which uses a relatively small number of meshes but includes the effects of turbulence flow around the perforated holes. The energy loss due to acceleration, retardation, turbulence, contraction, and expansion of the fluid as it approaches, passes, and leaves the perforated holes must be included in the formulation. The mathematical model and formulations developed must be validated by comparing the calculated results against the experimental data. Once they are validated, they can be use to study the effects of perforated dip plate in the HCDA analysis.

5. Dynamic Material Properties

Although computer codes can predict reasonably well the response of the containment under HCDA conditions, the code predictions can only be as good as the quality of the input data. Thus great care should be taken in defining input parameters. Among these parameters, the dynamic properties of the structural materials are quite important. They must be accurately defined in the input.

During the APRICOT code comparison, it was found that there was a lack of correlation in the pressure, impulse, and strain time histories between the code predictions and experimental data [8]. For example in APRICOT Problem No. 6, several codes predicted the two pressure loadings (direct incident and slug impact pressures) very well in shape and duration. Yet on examining the

strain histories, it is clear that all codes underpredicted the hoop strain arising from the first wave by significant amounts. Even the code which predicted the pressure nearly perfect underpredicted the strain by 30%. However, all of the codes then overpredicted the additional strain due to the second wave so that the resultant total strain is in much better agreement with measurement. It is true that the magnitude of those hoop strain are small, but this is not an argument which should be used to defend the computer codes since there can be many situations where the accurate prediction of strains of such magnitude may be crucial.

One possible explanation for this discrepancy is the incorrect material properties used in the analysis. In HCDA analysis, the reactor vessel wall is subjected to different types of loadings depending on the location. For example, at the mid-section of the reactor vessel, the wall is subjected first to an incident pressure load from the reactor core and then to an impact pressure load from the reactor cover. The strain rate of the wall deformation due to both pressure loads is relatively moderate. The wall at the upper portion of the reactor vessel wall is subjected to only slug impact loads, where the rate of deformation is considerably higher. Theoretically, the constitutive equations used in the analysis for structural materials should be able to reflect these differences. However, this is not the case in many current HCDA analyses, where only one set of stress-strain data with one strain rate is used for all calculations. Therefore, to improve the HCDA analysis, constitutive equations used in code calculations should be able to describe the behavior of the structural material under various dynamic loading conditions. To accomplish this, material tests must be performed so that effects of strain rate on flow stress and fracture strain can be determined. Other phenomena such as

yielding instabilities, Bauschinger effect, softening, and anisotropy induced by deformation should also be included in the constitutive equation.

Many dynamic tensile tests were performed under uniaxial and low to moderate strain rate conditions. These tests should be extended to dynamic biaxial loading conditions and high strain rates. Also methods must be developed so that results obtained on the small specimens can be applied to large structures.

6. Concrete Behavior Under High Temperature Conditions

Concrete behavior under high temperature is not well understood. Concrete structures in LMFBR plants may encounter high temperatures under accident conditions, such as sodium spillage and sodium fire. Under certain conditions the reaction of sodium with released moisture from concrete may even produce violent chemical reactions. In some extreme cases, concrete structures may be exposed to molten core materials. It is also known that when concrete is subjected to sudden high temperatures it may undergo spalling. In the case of sodium-concrete reactions, this becomes a very serious matter because it provides additional surface area for chemical reaction to take place. Thus, the understanding of the behavior of concrete structures subjected to either sustained high temperatures or chemical attack is vital to the design of safe and reliable LMFBR plants.

To achieve this, both tests and analytical studies are needed. Experiments will help to clarify the nature of sodium-concrete chemical reactions and to provide data on high-temperature concrete properties. Based on this information, mathematical models and computer codes can be developed. Once the mathematical models and computer codes are validated, they can be used to predict the behavior of concrete structures under accident conditions.

Two- and three-dimensional finite-element models and codes that can adequately predict the response of concrete structures to high temperatures must be developed. These codes and models should be applicable to the analysis of steel-lined equipment cells, reactor cavity structures, and the reactor containment building. They should be able to perform coupled heat transfer and stress analysis on concrete structures. A mathematical model that stimulates sodium-concrete reactions should be developed together with a concrete cracking model for high temperature and other hostile environments. The effects of moisture transport and pore pressure in concrete under high temperatures and creep and dilatation effects in heated concrete should be studied *both analytically and experimentally. Once these effects are determined,* they should be included in the mathematical model. It should be mentioned that the development of a good concrete cracking model is very important because the size of the crack opening is an important factor in the determination of the duration of the sodium-concrete reactions. For small size of cracks, the openings can be easily plugged up by the reaction products which prevent further reactions between sodium and concrete.

7. Multifield Containment Code

None of the containment codes developed considers multifield flows with interpenetrating fields. During an HCDA, reactor materials in the primary containment may move with different velocities, causing the materials to interpenetrate each other. One example of this is the entrainment and mixing of the sodium with the core materials. As a result, the phase of the material also undergoes changes from one state to another. Thus, containment codes, which do not permit the materials to interpenetrate and to change phase from one state to another, are inadequate. Multifield Eulerian containment code

with the capability of treating two phase flows must be developed for HCDA analysis. A complete set of conservation equations for the vapor phase as in IMF technique [9] or a reduced set of conservative equations as in the drift flux model [10] should be added to the existing set of conservation equations for computing the dynamic behavior of two-phase fluid mixture.

The value of multifield treatment is not in improving the evaluation of the response of vessel and reactor cover under accident conditions, but in providing insight into material mixing phenomena. If the mixing of two or three materials can be treated satisfactorily, it will prove useful for the calculations of heat transfer phenomena and for radiological studies during the HCDA. The heat transfer calculation will monitor energy losses thus reducing the energy available to perform destructive work on the reactor structures and components.

## 8. Prestressed Concrete Reactor Vessel (PCRV)

Utilization of the PCRV in LMFBRs may be necessitated by increasing licensing requirements due to speculated uncertainties. Current work on adaptation of the PCRV to LMFBR containment [11] indicates that the PCRV can exhibit substantially large energy absorption capability. Containment codes capable of treating PCRV structures should be developed.

## 9. Concluding Remarks

In conclusion, structural mechanics in fast reactor technology appears to have made significant progress. The computational methods and computer codes developed for HCDA analysis can predict reasonably well the response of the primary containment boundary system. The level of attainment at this time has been sufficient to provide the necessary input to design and safety evaluation

of LMFBR plants. What remains is the extension of this technology to reduce the conservatism in HCDA analysis and to provide more realistic models to reduce the cost of future LMFBR plants.

## Acknowledgments

This work is part of the Engineering Mechanics Program of the Reactor Analysis and Safety Division at ANL and was supported by the U.S. Department of Energy.

References

[1] A. V. Jones, "Coolant Cavitation in Dynamic Containment Loading," Nuclear Engineering and Design, 55 (12), pp. 151-292 (December 1979).

[2] Y. W. Chang and J. Gvildys, "Three-Dimensional Containment Code," Reactor Development Program Progress Report, ANL-RDP-84, pp. 2.59-2.6, Argonne National Laboratory (June 1979).

[3] T. Belytschko and R. Mullen, "Two-Dimensional Fluid-Structure Impact Computations with Regularization," Computer Methods in Applied Mechanics and Engineering, 27 (1981).

[4] M. L. Wilkins, R. E. Blum, E. Cronshagen, and P. Granthan, "A Method for Computer Simulation of Problems in Solid Mechanics and Gas Dynamics in Three Dimensions and Time," UCRL-51574, Rev. 1, Lawrence Livermore Laboratory (May 1975).

[5] D. Kosloff and G. A. Frazier, "Treatment of Hourglass Patterns in Low Order Finite Element Codes," International Journal for Numerical and Analytical Methods in Geomechanics, Vol. 2 (1978).

[6] D. P. Flanagan and T. Belytschko, "A Uniform Strain Hexahedron and Quadrilateral with Orthogonal Hourglass Control," International Journal for Numerical Methods in Engineering, Vol. 17 (1981).

[7] C. Y. Wang, W. R. Zeuch, and Y. W. Chang, "ALICE Improvement," Liquid Metal Fast Breeder Reactor Technical Progress Report, ANL-RDP-101, pp. 1.77-1.78, Argonne National Laboratory (January-March 1981).

[8] N. E. Hoskin, "APRICOT Code Comparisons - Results of Phase 2," AWRE/44/92/17, FREC/P(79)29 (March 1980).

[9] F. H. Harlow and A. A. Amsden, "Numerical Calculation of Multiphase Fluid Flow," Journal of Computational Physics, pp. 19-52 (1975).

[10] C. W. Hirt and T. A. Oliphant, "SOLA-PLOOP: A Non-Equilibrium, Drift Flux Code for Two-Phase Flow in Networks," Proceedings of the Specialists Meeting on Transient Two-Phase Flow, Toronto, Ontario, Canada (August 1976).

[11] A. H. Marchertas, "Analysis and Application of Prestressed Concrete Reactor Vessel for LMFBR Containment," Nuclear Engineering and Design, 49, Nos. 1 and 2, pp. 155-173 (July 1978).

Table 1

Comparison of 2-D and 3-D Slug Impact Problem

| Items | 2-D | 3-D |
|---|---|---|
| Total No. of Meshes | 6 x 12 = 72 | 27 x 12 = 324 (90° sector) |
| No. of Shell Elements | 12 | 144 |
| No. of Mesh Points | 91 | 481 |
| No. of Bytes Per Mesh | 160 | 428 |
| IBM 370 CPU Time Per Cycle | .07 sec | 2.608 sec |

8 IBM 370 Bytes $\tilde{=}$ 1 CDC 7600 Machine Word

## Figure Captions

Fig. 1. Comparison of Pressure Histories Obtained with Implicit and Explicit Time Integration Schemes.

Fig. 2. Sector Model of a Pool Reactor.

Fig. 3. Hexahedral Hourglass Modes in the $\xi$-direction. (a) Mode 1, (b) Mode 2, (c) Mode 3, (d) Mode 4.

Fig. 4. Mathematical Model of a Reactor.

Fig. 5. Configurations of the Reactor with the Perforated Dip Plate.

Fig. 6. Configurations of the Reactor without the Perforated Dip Plate.

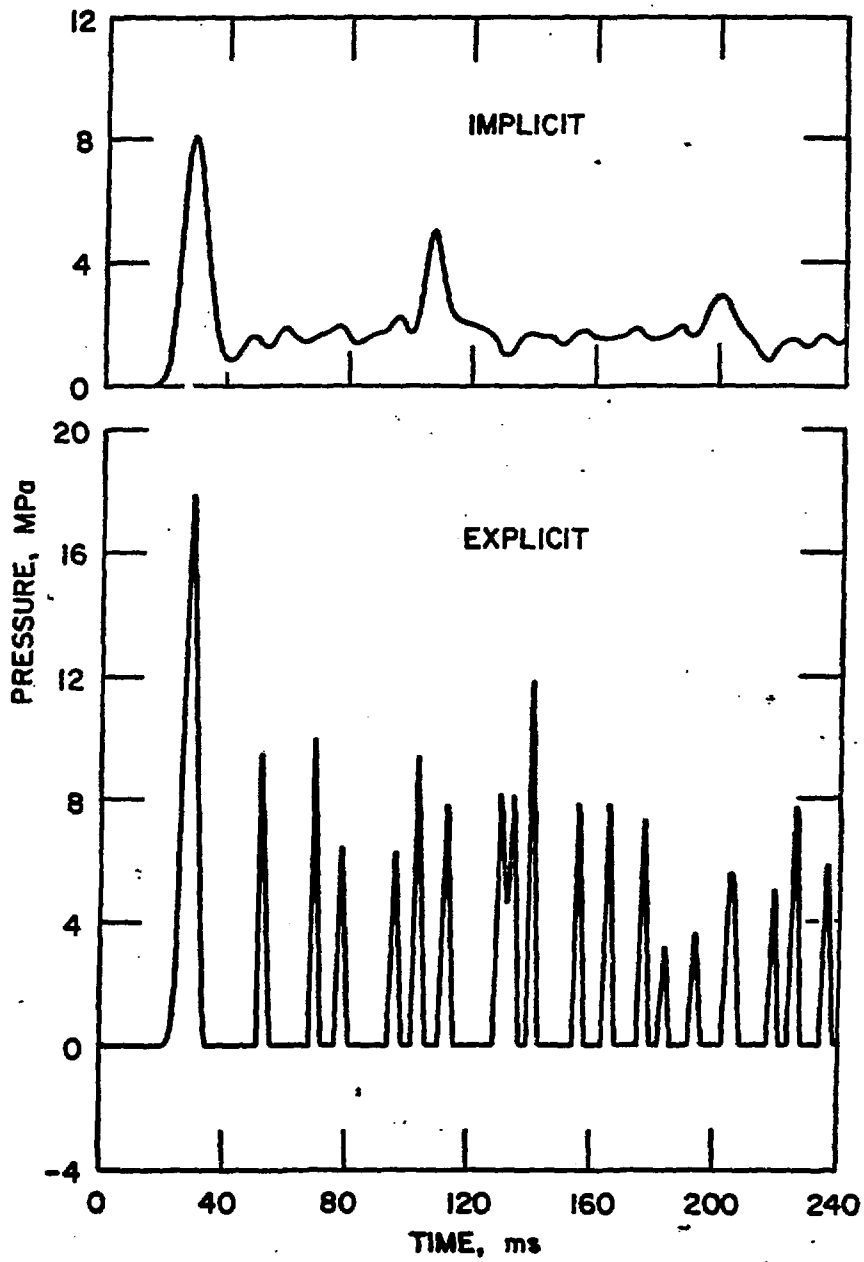


Fig. 1. Comparison of Pressure Histories Obtained with Implicit and Explicit Time Integration Schemes.

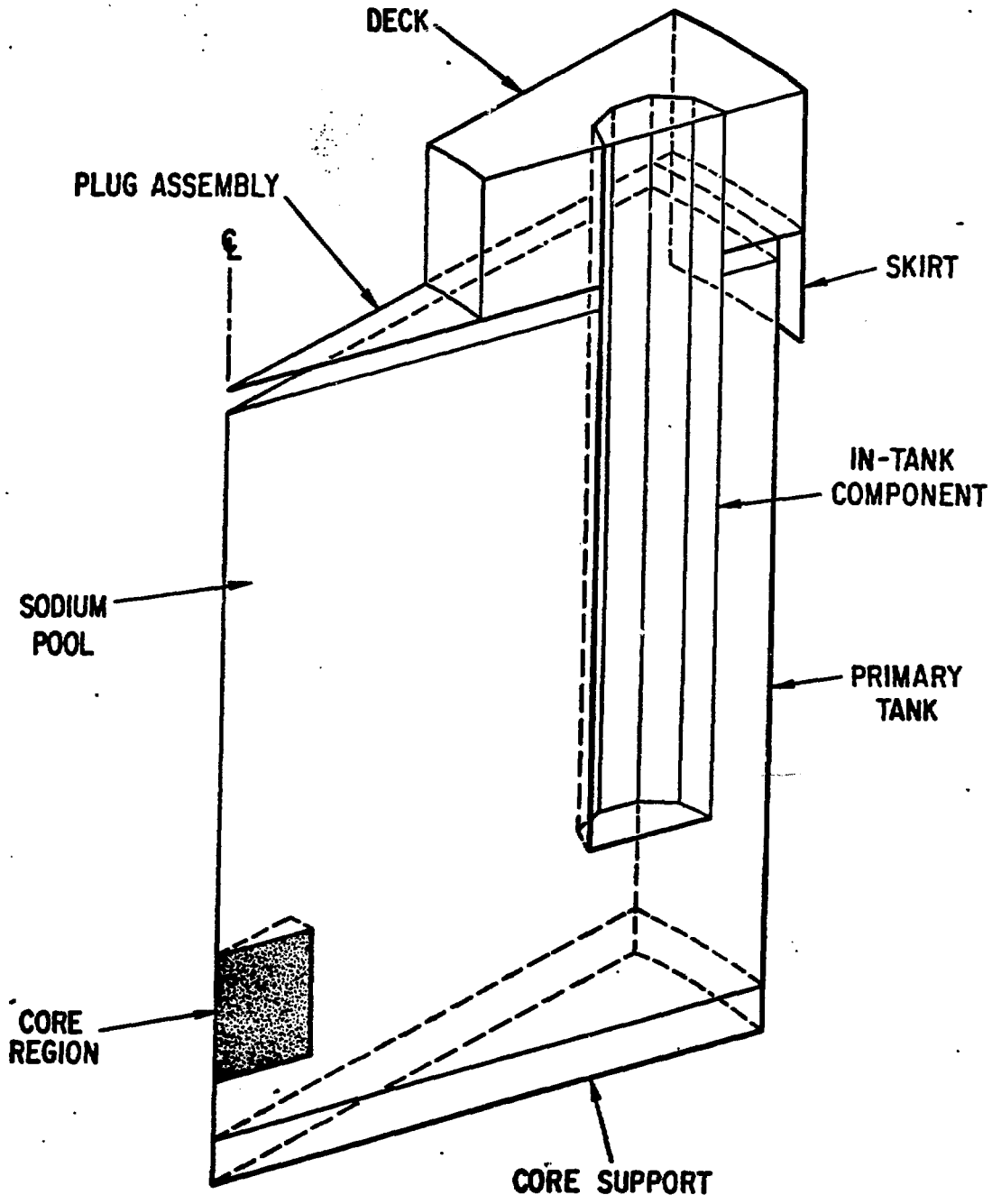


Fig. 2. Sector Model of a Pool Reactor.

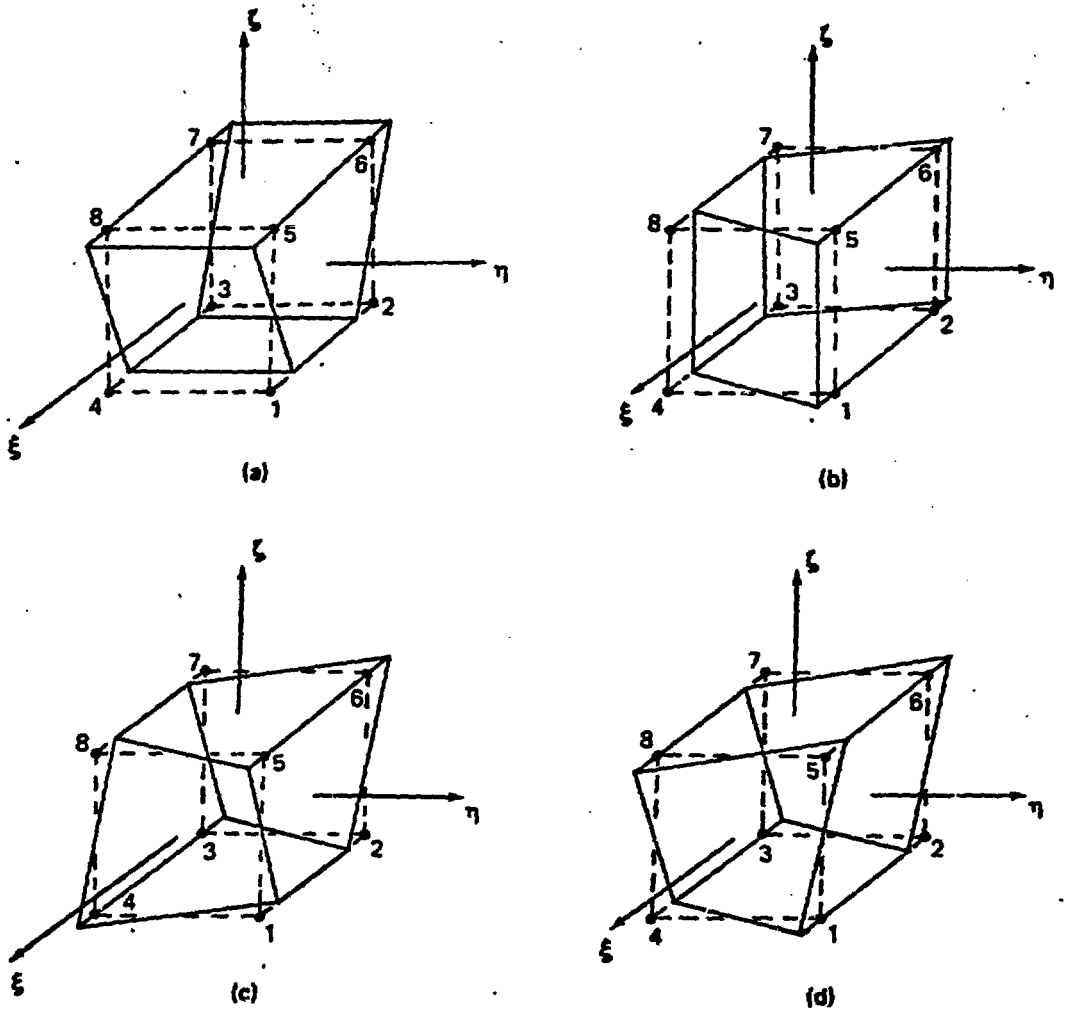


Fig. 3. Hexahedral Hourglass Modes in the ξ-direction. (a) Mode 1, (b) Mode 2, (c) Mode 3, (d) Mode 4.

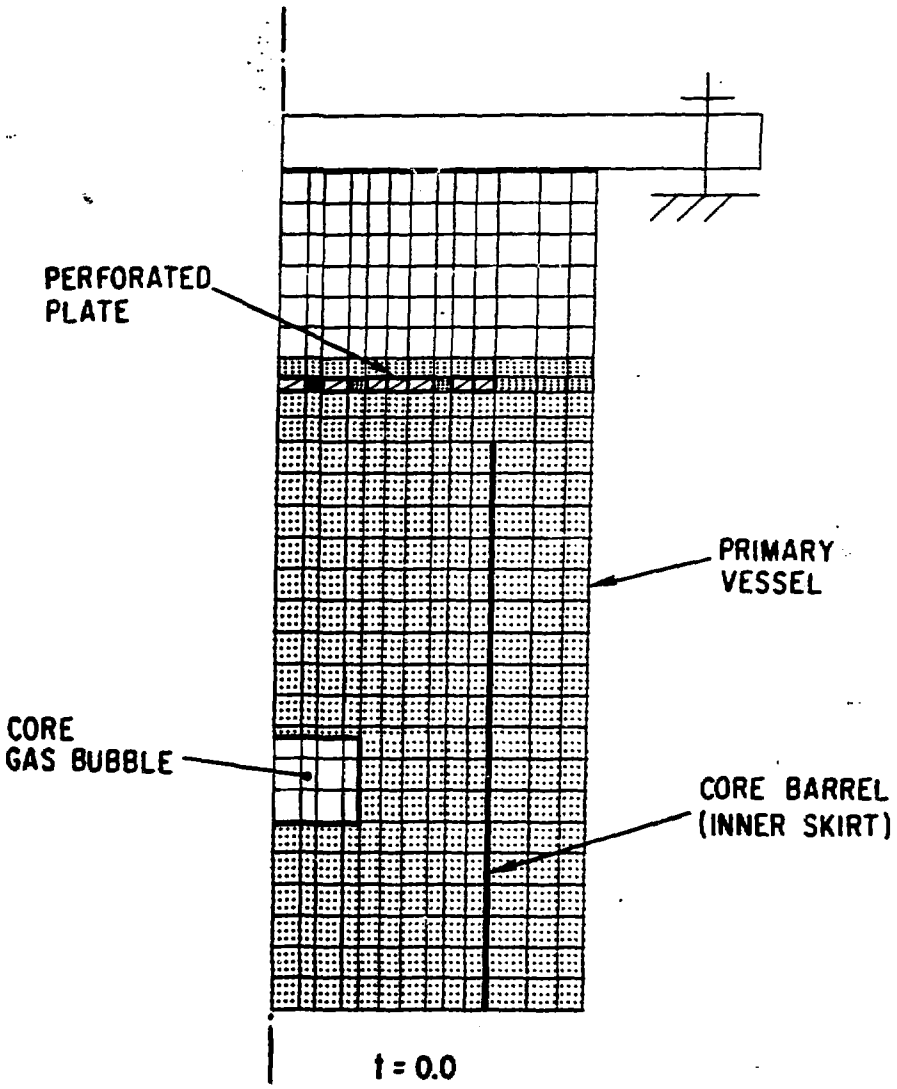


Fig. 4. Mathematical Model of a Reactor.

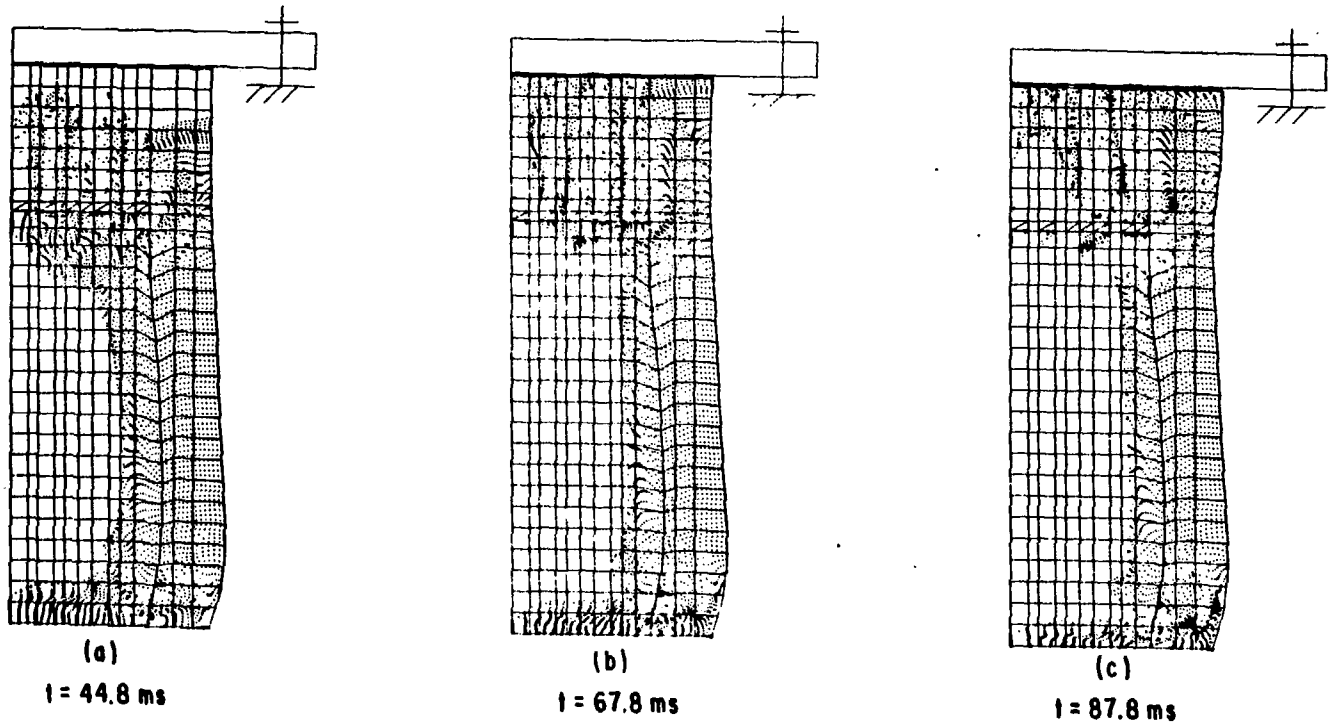


Fig. 5. Configurations of the Reactor with the Perforated Dip Plate.

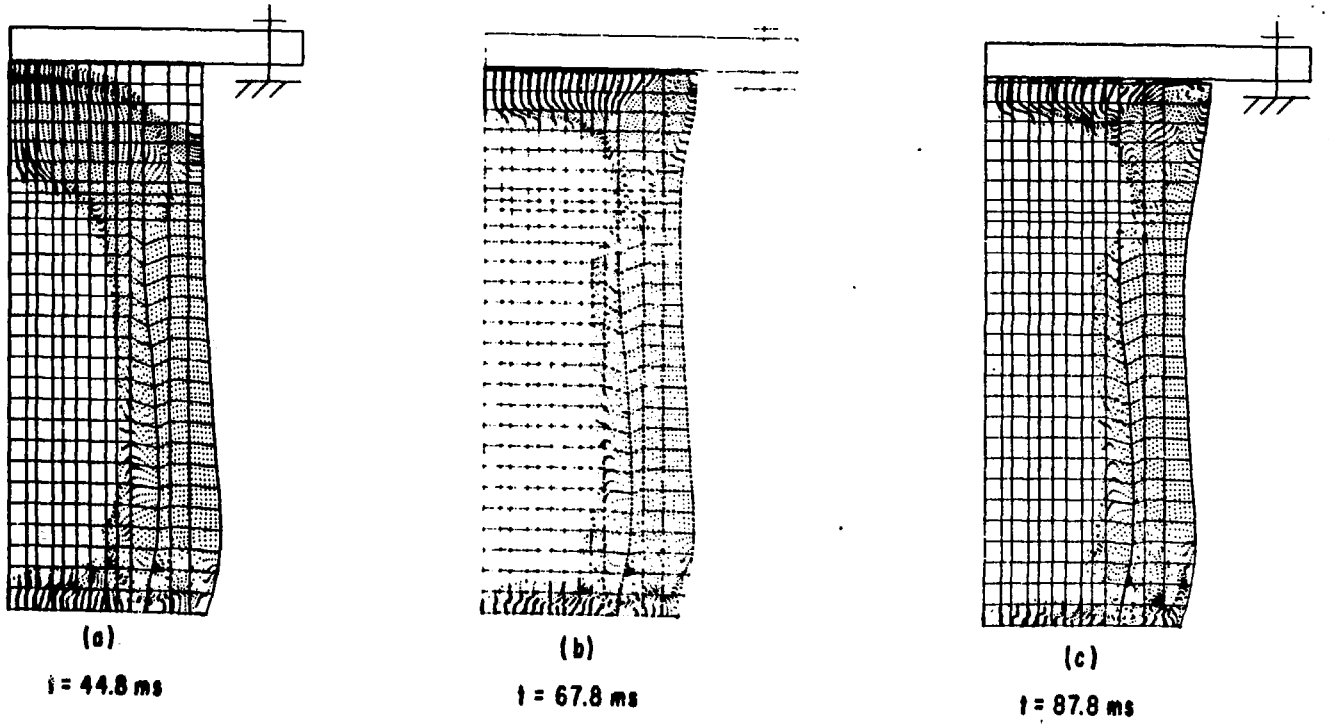


Fig. 6. Configurations of the Reactor without the Perforated Dip Plate.

## DISCLAIMER